

Towards the continuum coupling in nuclear lattice effective field theory I: A three-particle model

J.-J. Wu^{*1} and Ulf-G. Meißner^{†2,3,4}

¹*School of Physical Sciences, University of Chinese Academy of Sciences, Beijing 100049, China*

²*Helmholtz-Institut für Strahlen- und Kernphysik and Bethe Center for Theoretical Physics, Universität Bonn, D-53115 Bonn, Germany*

³*Institute for Advanced Simulation, Institut für Kernphysik, and Jülich Center for Hadron Physics, Forschungszentrum Jülich, D-52425 Jülich, Germany*

⁴*Tbilisi State University, 0186 Tbilisi, Georgia*

Abstract

Weakly bound states often occur in nuclear physics. To precisely understand their properties, the coupling to the continuum should be worked out explicitly. In a first step, we use a simple nuclear model in the continuum and on a lattice to investigate the influence of a third particle on a loosely bound state of a particle and a heavy core.

* wujiajun@ucas.ac.cn

† meissner@hiskp.uni-bonn.de

I. INTRODUCTION

Along the nuclear chart, there are a number of weakly bound states like in case of halo nuclei or for isotopes close to the drip lines. These states are characterized by binding energies in the keV range rather than the few MeV typical for nuclear binding. Such loosely (or weakly) bound states are thus closely located to decay thresholds and the corresponding continuum of states. Under such circumstances the coupling of such a bound state to the continuum can no longer be neglected, for reviews see e.g. [1–3]. For conventional nuclear models, like e.g. the shell model or the no-core-shell model, the coupling to the continuum based e.g. on Berggren’s representation [4, 5], that treats bound, resonant and continuum states on the same footing, is well established, see e.g. [6–8]. In addition, *ab initio* calculation for systems such as ${}^4\text{He}+n+n$ and $A = 7$ isotopes have been performed including continuum effects [9–11].

Nuclear lattice effective field theory (NLEFT) is a novel method for performing *ab initio* calculations in nuclear structure and reaction physics [12, 13]. The basic idea is to discretize space-time on a finite volume $L^3 \times L_t$, with L (L_t) the spatial (temporal) size. Nucleons are placed on the lattice sites and their interaction are given in terms of properly modified chiral potentials, consisting of pion exchanges and short-distance operators. Strong isospin-breaking effects and the long-ranged Coulomb potential are also included, leading to a number of intriguing results, like e.g. the *ab initio* calculation of the Hoyle state in ${}^{12}\text{C}$ [14] or the first microscopic calculation of low-energy α - α scattering [15]. What is missing in this framework is the coupling to the continuum. Of course, on the lattice we have only real-valued energies, so a direct application of the Berggren approach is not possible. However, as shown by Lüscher in this seminal work, the complex-valued scattering phase shift can be mapped onto the volume-dependence of the lattice energy levels [16, 17]. We seek a similar formalism to explicitly describe the continuum coupling.

In this work, we use a simple model of a heavy core A coupled to one or two nucleons N , as described in Sect. II. In Sect. III we consider $AN \rightarrow AN$ scattering and adjust the AN interaction such that a very weakly bound state emerges. Using the Hamiltonian formalism of Refs. [18–24] we calculate the energy levels of this system in a finite volume. The full ANN system is considered in Sect. IV, where we adjust the parameters so that there is no three-particle bound state and we can thus study the influence of the unbound third particle

on the AN scattering matrix. We conclude with a summary and outlook in Sect. V. The Appendix contains a short discussion of the normalization of the scattering equation used.

II. THE MODEL

Consider a three-particle model (ANN system), with the mass of the A particle about 10 times the mass of the N particle with mass m . The A particle thus mimics the nuclear core. To be specific, let us calculate $AN \rightarrow AN$ scattering. For simplicity, we use a separable potential of the form

$$V_H^{AN}(p, p') = \frac{1}{\sqrt{2\omega_A(p)2\omega_N(p)}} g f(p, \Lambda) f(p', \Lambda) \frac{1}{\sqrt{2\omega_A(p)2\omega_N(p)}}, \quad (1)$$

with the regulator function

$$f(p, \Lambda) = \frac{\Lambda^2}{p^2 + \Lambda^2}, \quad (2)$$

with $\omega_i(q) = \sqrt{m_i^2 + q^2}$ and g is the coupling constant. The normalization is explained in the Appendix. In what follows, we set $m_A = 10 \text{ GeV}$, $m = \Lambda = 1 \text{ GeV}$. We are interested in the case that the AN system has a very weakly bound state B with keV binding energy, so the coupling g will be tuned accordingly.

Then we can construct the Hamiltonian in the finite volume and find its eigenvalues [19]. The Hamiltonian matrix is defined as follows:

$$H = H_0 + H_I,$$

$$(H_0)_{ij} = \delta_{ij} (\omega_A(k_i) + \omega_N(k_i)), \quad (3)$$

$$(H_I)_{ij} = \frac{\sqrt{C_3(i)C_3(j)}}{4\pi} \left(\frac{2\pi}{L}\right)^3 V_H(E, k_i, k_j), \quad (4)$$

where $k_i = \sqrt{i}2\pi/L$ and $C_3(i)$ represents the number of ways to sum the square of the three integers to equal i . Further, the factor $(\sqrt{C_3(i)C_3(j)})/(4\pi)(2\pi/L)^3$ is due to the quantization in a finite box with size L as explained in Refs. [18, 19].

For the full ANN system with a fixed total momentum, we have two free momenta. This will lead to a Hamiltonian matrix in the finite volume with a huge dimension. For simplification, we thus consider the BN system instead of ANN , that means we use a version of the dimer approximation, see e.g. [25], reminiscent of the so-called Faddeev fixed center approximation, see e.g. Refs. [26, 27]. We thus consider the scattering process $BN \rightarrow BN$.

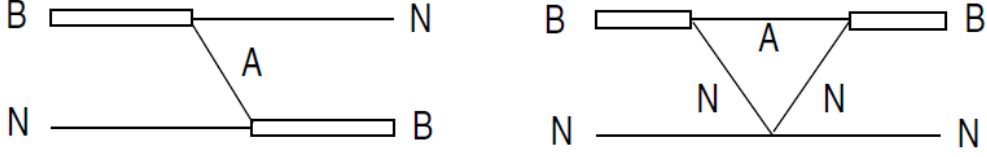


FIG. 1: Effective diagrams for the $BN \rightarrow BN$ process

The left diagram of Fig. 1 shows the attractive interaction between B and N since the AN system has a weak attractive interaction. To calculate this diagram, we need to get the coupling of $B \rightarrow AN$ process. Since the B is a loosely bound state of AN , one gets the coupling from the amplitude of $AN \rightarrow AN$ around the pole position of B as follows,

$$T_H^{AN}(E \sim m_B, q = q_0(E), q' = q_0(E)) = \frac{1}{2m_A} \frac{1}{2m_N} 4\pi \frac{\tilde{g}^2}{2m_B(E - m_B)}, \quad (5)$$

where $q_0(E)$ is the on-shell momentum with energy E , and T_H^{AN} is obtained from Eq.(22) with the potential V_H^{AN} . The factor $1/(2m_A) \cdot 1/(2m_N)$ originates from the the difference between V_H and V_L (see the Appendix), the momentum is on-shell, so it is close to the mass of the particle, and the factor 4π is from the angular integration, since we only consider the s-wave. Further, the coupling \tilde{g} has dimension energy. With that, the potential of $BN \rightarrow BN$ from A -exchange takes the form

$$V_H^{BN1}(p, p') = \frac{2\pi}{\sqrt{2\omega_B(p)2\omega_N(p)}} \times \int d\cos\theta \frac{\tilde{g}^2}{(E_A^2) - (\vec{p} - \vec{p}')^2 - m_A^2} \frac{1}{\sqrt{2\omega_B(p')2\omega_N(p')}} , \quad (6)$$

$$E_A^2 = \frac{1}{2} ((\omega_B(p) - \omega_N(p'))^2 + (\omega_N(p) - \omega_B(p'))^2) . \quad (7)$$

Since our potential should be independent of the total energy, we take the average of the two processes $B \rightarrow AN$ and $NA \rightarrow B$. Next, we need to pick out the s-wave contribution of this diagram, so we perform the angular integration between \vec{p} and \vec{p}' . At last, the equation for the potential takes the form

$$V_H^{BN1}(p, p') = \frac{\tilde{g}^2}{\sqrt{2\omega_B(p)2\omega_N(p)2\omega_B(p')2\omega_N(p')}} \frac{\pi}{pp'} \times \ln \left(\frac{m_B^2 + m_N^2 - m_A^2 - (\omega_B(p)\omega_N(p') + \omega_N(p)\omega_B(p')) + 2pp'}{m_B^2 + m_N^2 - m_A^2 - (\omega_B(p)\omega_N(p') + \omega_N(p)\omega_B(p')) - 2pp'} \right) . \quad (8)$$

Note that this potential should be negative, because in Eq. (6) the propagator of the exchanged A particle is negative.

Now let us consider the contribution from the right diagram of Fig. 1. This includes a triangle loop, and the main interaction is the $NN \rightarrow NN$ interaction. First, the $NN \rightarrow NN$ interaction can be written as,

$$V_H^{NN}(p, p') = \frac{1}{\sqrt{2\omega_N(p)}2\omega_N(p)} g_{NN} f(p, \Lambda) f(p', \Lambda) \frac{1}{\sqrt{2\omega_A(p)}2\omega_N(p)}, \quad (9)$$

where the regulator function is chosen the same as for the AN interaction. In this model, we want to describe the situation that BN system can not form a bound state, therefore the coupling g_{NN} is only parameter which allows to achieve that.

Next, we work out the potential based on the diagram on the right side of Fig. 1:

$$V_H^{BN^2}(p, p') = \frac{2\pi}{\sqrt{2\omega_B(p)}2\omega_N(p)} \int d\cos\theta V_L^{BN^2}(\vec{p}, \vec{p}') \frac{1}{\sqrt{2\omega_B(p')}2\omega_N(p')}, \quad (10)$$

where

$$\begin{aligned} V_L^{BN^2}(\vec{p}, \vec{p}') &= \int d^4q \tilde{g}^2 \frac{1}{q_0^2 - \vec{q}^2 - m_A^2} \frac{1}{(\omega_B(p) - q_0)^2 - (\vec{p} - \vec{q})^2 - m_N^2} \\ &\times \frac{1}{(\omega_B(p') - q_0)^2 - (\vec{p}' - \vec{q})^2 - m_N^2} T_{NN}^L \\ &= \int d^3\vec{q} \tilde{g}^2 \frac{1}{2\omega_A(q)} \frac{1}{(\omega_B(p) - \omega_A(q))^2 - (\vec{p} - \vec{q})^2 - m_N^2} \\ &\times \frac{1}{(\omega_B(p') - \omega_A(q))^2 - (\vec{p}' - \vec{q})^2 - m_N^2} T_L^{NN}, \end{aligned} \quad (11)$$

where T_L^{NN} is the amplitude of $NN \rightarrow NN$. In the calculation of T_L^{NN} , we make some further assumptions. First, we assume $T_L^{NN} \sim V_L^{NN}$, which should be acceptable as we are not interested in the detailed structure of the NN scattering amplitude. Also, we require this interaction in a boosted frame. Although the form of V_L is not Lorentz invariant, we can rewrite the potential in a special form and define all inputs the center-of-mass (CM)

system. This means that we write V_L^{NN} as

$$T_L^{NN} \sim V_L^{NN} = g_{NN} f(k^*, \Lambda) f(k'^*, \Lambda), \quad (12)$$

$$k^{*2} = E_{NN}^2/4 - m_N^2, \quad (13)$$

$$E_{NN}^2 = \left(\sqrt{(\vec{q} - \vec{p})^2 + m_N^2} + \sqrt{\vec{p}^2 + m_N^2} \right)^2 - q^2, \quad (14)$$

$$k'^{*2} = E'_{NN}{}^2/4 - m_N^2, \quad (15)$$

$$E'_{NN}{}^2 = \left(\sqrt{(\vec{q} - \vec{p}')^2 + m_N^2} + \sqrt{\vec{p}'^2 + m_N^2} \right)^2 - q^2. \quad (16)$$

Then at last we can get V_H^{BN2} as defined in Eq.(10-16) as follows:

$$V_H^{BN2}(p, p') = \frac{4\pi^2}{\sqrt{2\omega_B(p)2\omega_N(p)2\omega_B(p')2\omega_N(p')}} \int q^2 dq \frac{\tilde{g}^2 g_{NN}}{2\omega_A(q)} H(p, q) H(p', q), \quad (17)$$

where

$$H(p, q) = \int d\cos\theta \frac{1}{m_B^2 + m_A^2 - m_N^2 - 2\omega_B(p)\omega_A(q) + 2pq\cos\theta} \times \frac{4\Lambda^2}{\left(\sqrt{q^2 + p^2 - 2pq\cos\theta + m_N^2} + \sqrt{p^2 + m_N^2} \right)^2 - q^2 - 4m_N^2 + 4\Lambda^2}, \quad (18)$$

which can easily be evaluated numerically.

III. RESULTS FOR $2 \rightarrow 2$ SCATTERING

First, we must fix the coupling constant g . In the left panel of Fig. 2, we show the binding energy of the two-particle system as a function of the coupling g . The latter is chosen in a range so that the binding is weak, and indeed at $g = -30.65$, there is no more bound state. In what follows, we choose $g = -31.0$, for which one finds a loosely bound state at $|E_B| = 11.15$ keV. In the right panel of Fig. 2, the corresponding scattering phase shift in the close-to-threshold region is shown, it exhibits the typical features of a weakly bound state close to threshold.

The corresponding energy levels in the finite volume are shown in Fig. 3. The bound state level is clearly visible, its bending downwards for smaller lattice sizes is an expected finite volume effect. For sufficiently large L , these finite volume effects are visibly absent.

It is also instructive to compare our formalism with the Lüscher equation [16, 17]. For that, we pick out 17 energy levels at $L = 10$ fm, and then we use following Lüscher equation

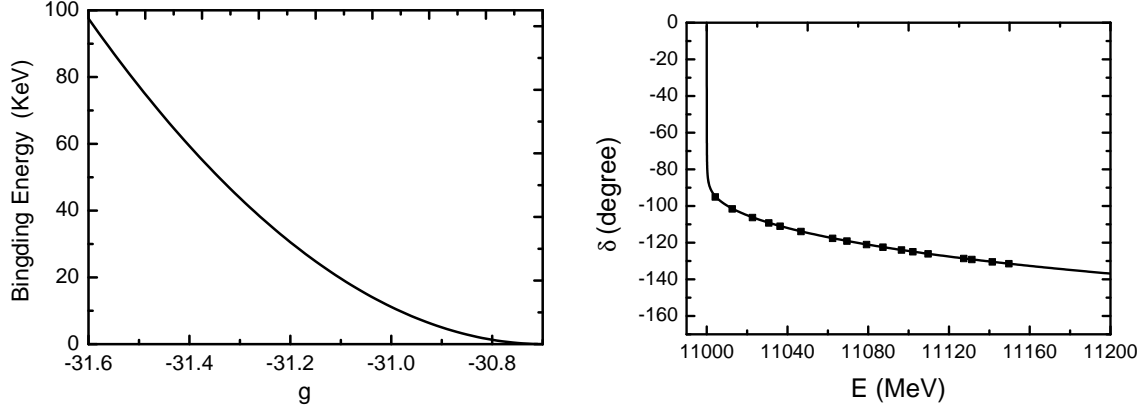


FIG. 2: Left panel: Binding energy of the AN system as a function of the coupling constant g . Right panel: Phase shift for $AN \rightarrow AN$ scattering for $g = -31.0$. The black points are calculated from the corresponding energy levels depicted in Fig. 3 using the Lüscher equation.

to calculate the phase shifts from the corresponding energy levels,

$$\delta(q_E) = \tan^{-1} \left(\frac{q_E L \sqrt{\pi}}{2\mathcal{Z}(1; (\frac{q_E L}{2\pi})^2)} \right) + n\pi \quad (19)$$

where q_E is on-shell momentum corresponding to the energy E ,

$$q_E = \frac{E}{2} \sqrt{\left(1 - \left(\frac{m_N + m_A}{E}\right)^2\right) \left(1 - \left(\frac{m_N - m_A}{E}\right)^2\right)}, \quad (20)$$

and $\mathcal{Z}(1; q^2)$ is well known Zeta-function. After regularization it can be calculated as follows,

$$\begin{aligned} \mathcal{Z}(1; q^2) &= \sum_{\vec{n} \in \mathbb{Z}^3} \frac{1}{\vec{n}^2 - q^2} \\ &= -\frac{1}{q^2} - 8.91363292 + 16.53231596q^2 + \sum_{\vec{n} \in \mathbb{Z}^3} \frac{q^4}{\vec{n}^4 (\vec{n}^2 - q^2)}. \end{aligned} \quad (21)$$

We find that the so calculated phase shifts are all on the phase shift curve calculated directly from the scattering function, see Fig. 2. This shows that our calculation is consistent with the Lüscher equation.

IV. RESULTS FOR THE FULL SYSTEM

Before showing the results, a few remarks are in order. We note that the attractive potential of $BN \rightarrow BN$ by A -exchange will have a sizeable magnitude at threshold, because

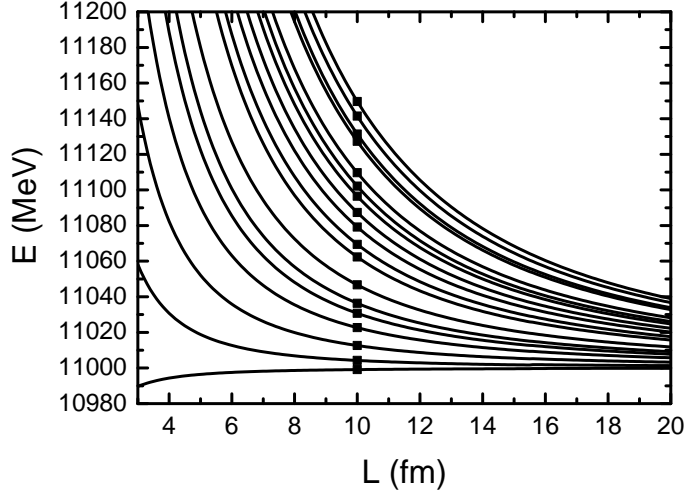


FIG. 3: Energy levels for the weakly bound AN system in a finite volume L^3 . The meaning of the black squares at $L = 10$ fm is explained in text, the also Fig. 2.

the propagator of the A -particle will be very close to zero since B is a loose bound state of AN . Similarly, the repulsive potential $BN \rightarrow BN$ generated by the triangle-loop will also have a large value close to the threshold, since at that time, both nucleons can be to their mass shell. We will therefore consider various choices to adjust the coupling g_{NN} , cf. Eq. (9). One is that these two contributions cancel exactly at threshold (case 1) and the other corresponds to the case that the total potential is repulsive (case 2). In Fig. 4 we show the potential for various choices of the coupling g_{NN} .

Case 1: With $g_{NN} = 48.34$, there is a repulsive interaction between $BN \rightarrow BN$, but at threshold, the potential is just zero. Above threshold the potential increases fast and then drops almost with the same slope as the potential from the loop. Then from this potential, the corresponding finite volume spectrum can be computed as shown in the left panel Fig.5. It is surprising that there is still a energy level below the threshold of BN system since there is pure repulsive potential. This is due to the strange structure of potential at the threshold: At threshold, the potential is exactly zero, and therefore the first term of full Hamiltonian matrix in the finite volume is just the sum of the masses of B and N . On the other hand, in the finite volume the momentum is discrete, therefore, the off-diagonal term in the Hamiltonian matrix will provide an attractive potential weather the original potential is attractive or repulsive. Combing these two factors, the first energy level will be lower

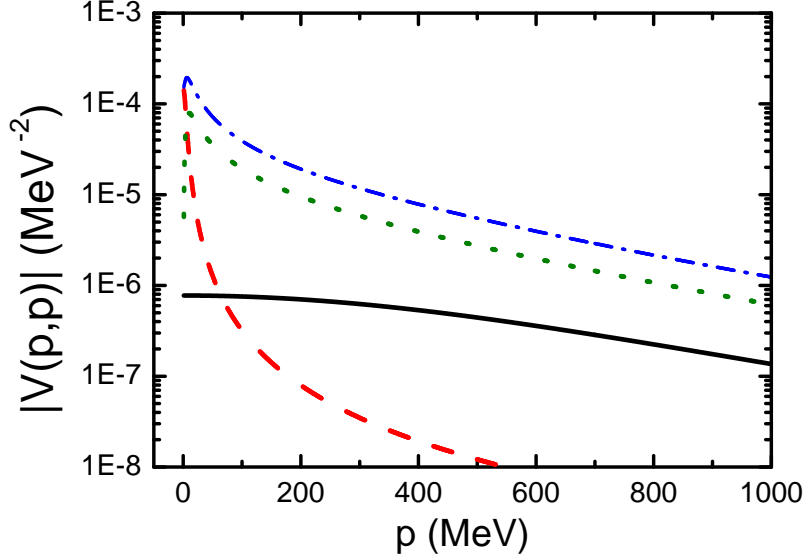


FIG. 4: Potentials in the AN (black solid line) and the BN system. In the latter case, two choices for the coupling g_{NN} are made as discussed in the text (blue dash-dotted and green dotted lines). The red dashed line shows the attractive BN potential from A -exchange.

than the threshold in the finite volume, especially for small lattice size. The corresponding phase shift for $BN \rightarrow BN$ is shown in the right panel of Fig. 5. It is almost the same as that in AN scattering, but we note that in the region very close to the threshold the phase is increasing to about 10° as shown in the inset of right panel of Fig. 5. The steep fall-off of the phase can be traced back to the fast decrease of the potential, as shown by the green dotted curve in Fig. 4. We also check our method in comparison to the Lüscher equation here. The black points in the phase shift figure are calculated from the energy levels at $L = 10$ fm which are shown as black points in the left panel of Fig.5. Within small fluctuations, all of the points are consistent with the curves of phase shift which directly calculated from scattering function. These fluctuations will be discussed in the next case.

Case 2: With $g_{NN} = 96.68$, there is a repulsive interaction and even at the threshold it has a large value, although it still increases slightly with energy, see the blue dash-dotted line in Fig. 4. There is no bound state below the threshold in the finite volume spectrum as shown in the left panel of Fig. 6. In this case, the phase shift has a similar behaviour to that in the case 1 in the threshold region, but the magnitude is much smaller, the largest phase shift here is around 1° . This corresponds to a potential barrier, so that the phase

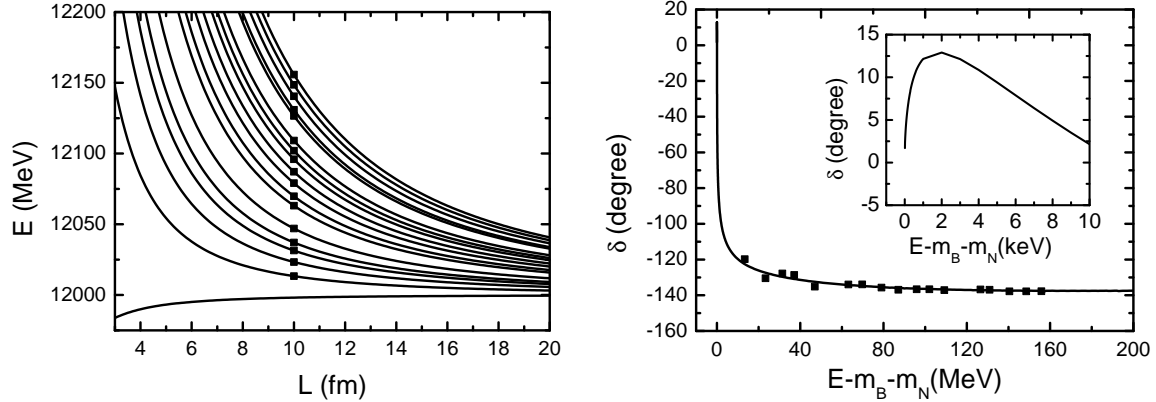


FIG. 5: Left panel: Energy levels for the BN system in a finite volume L^3 for $g_{NN} = 48.34$. Right panel: Phase shift for $BN \rightarrow BN$. The inset shows the phase shift very close to threshold. The black points in the left panel are the data at $L = 10$ fm. The black points in the right panel are calculated from the corresponding data in the left panel with $L = 10$ fm by using the Lüscher equation as shown in Eq. (19).

almost does not increase and very quickly starts to fall as fast as the case 1, shown as the blue dash-dotted curve in Fig. 4. Analogous to case 1, we also check the consistency with Lüscher equation. From the left panel of Fig. 6, the first four points are far away from the curve of the phase shift, which means that there is some inconsistency at the low energy levels. Actually, our method has a systematic difference with the Lüscher equation, which is the difference between summation and interaction of a regular function as shown in the appendix of Ref. [19]. This difference would be large when the regular function has some sharp structure and it is proportional to $\exp(-Lm)$, where m is the scale corresponding to the variation of the potential close to threshold. In our case, the potential contributes significantly to the regular function and is very quickly varying around the threshold, therefore, such difference between summation and integration will be very large in this case. However, in the $A + N \rightarrow A + N$ case, the potential is much more flat, and this leads perfect consistency between our method and the Lüscher equation as shown in the left panel of Fig. 2. In other words, the fine structure at the threshold will be missing in the finite volume, when a too small volume is used. It can be resolved by increasing the lattice size, as shown in Fig. 6. The red circles are for the larger volume $L = 17$ fm and are well consistent with the phase curve. Therefore, in principle, our method is consistent with

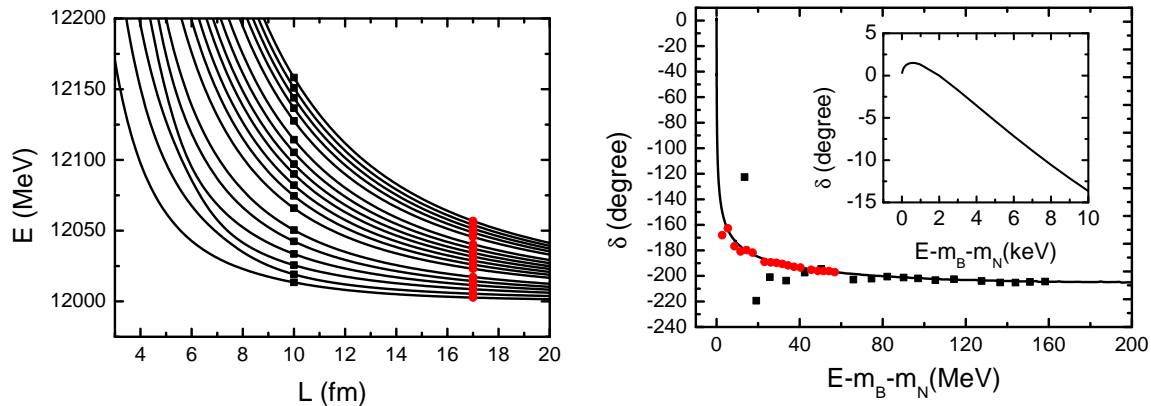


FIG. 6: Left panel: Energy levels for the BN system in a finite volume L^3 for $g_{NN} = 96.68$. Right panel: Phase shift for $BN \rightarrow BN$. The inset shows the phase shift very close to threshold. The black points and red circles in the left panel are the data at $L = 10$ fm and 17 fm, respectively. The black points and red circles in the right panel are calculated from the corresponding data in the left panel with $L = 10$ fm and 17 fm, respectively, using the Lüscher equation as shown in Eq. (19).

Lüscher equation.

From these observation we speculate that refined calculations will make it possible to find a compact formula for the influence of the continuum on a weakly bound state on the lattice.

V. SUMMARY AND OUTLOOK

In this letter, we have made a first step to evaluate the influence of the continuum on weakly bound states. We have shown that there is a visible interplay between the weak bound state B in the two-particle system and the third particle, which leaves its traces in the lattice energy spectrum. To draw more definite conclusions, the model used requires much refinement. In a first step, the full three-body ANN system should be investigated. Since the thresholds of BN and ANN are very close, we expect that the inelastic effects due to breakup reaction $B + N \rightarrow A + N + N$ will affect the spectrum. Then, the interaction potentials have to be refined so that they resemble more closely the nuclear case. Also, higher partial waves need to be included. Work along these lines is under way.

Acknowledgments

We thank Dean Lee for a useful communication. We acknowledge partial financial support from the Deutsche Forschungsgemeinschaft (SFB/TRR 110, ‘‘Symmetries and the Emergence of Structure in QCD’’, grant no. TRR 110), by the Chinese Academy of Sciences (CAS) President’s International Fellowship Initiative (PIFI) (grant no. 2018DM0034) , by VolkswagenStiftung (grant no. 93562) and by the Fundamental Research Funds for the Central Universities.

Appendix: Normalization of the scattering equation

Here, we briefly discuss the normalization of our scattering T-matrix. This normalization is similar to the formalism used in Ref. [28]. Consider the s-wave of the process $AN \rightarrow AN$, with the scattering function given by

$$T_H(E, |\vec{k}|, |\vec{k}'|) = V_H(|\vec{k}|, |\vec{k}'|) + \int q^2 dq V_H(|\vec{k}|, q) \frac{1}{E - \omega_A(q) - \omega_N(q) + i\epsilon} T_H(E, q, |\vec{k}'|) , \quad (22)$$

where $\omega_i(q) = \sqrt{m_i^2 + q^2}$. Correspondingly, in the Bethe-Salpeter function, where k, k' are four-momenta, takes the form

$$T_L(P, k, k') = V_L(P, k, k') + \int d^4q V_L(P, k, q) \frac{1}{q^2 - m_A^2 + i\epsilon} \frac{1}{(P - q)^2 - m_N^2 + i\epsilon} T_L(P, q, k') . \quad (23)$$

Actually, Eq. (22) can be recognized as the three-dimensional reduction of Eq. (23) by using

$$\int d^4q \frac{1}{q^2 - m_A^2 + i\epsilon} \frac{1}{(P - q)^2 - m_N^2 + i\epsilon} \sim \int q^2 dq \frac{1}{E - \omega_A(q) - \omega_N(q) + i\epsilon} \frac{1}{2\omega_A(q)2\omega_N(q)} . \quad (24)$$

Therefore, we can get the relationship between the V_H and V_L ,

$$V_H(E, |\vec{k}|, |\vec{k}'|) = \frac{2\pi}{\sqrt{2\omega_A(k)2\omega_N(k)}} \int d \cos \theta V_L(P, k, k') \frac{1}{\sqrt{2\omega_A(k')2\omega_N(k')}} . \quad (25)$$

Note that we have been cavalier with some factors, such as $(2\pi)^n$, since these will be absorbed into the coupling in V_L . Also, this equation is the simple form of Eqs.(23-24) of Ref. [28].

-
- [1] J. Dobaczewski, N. Michel, W. Nazarewicz, M. Ploszajczak and J. Rotureau, Prog. Part. Nucl. Phys. **59** (2007) 432 [arXiv:nucl-th/0701047 [nucl-th]].
 - [2] N. Michel, W. Nazarewicz, M. Ploszajczak and T. Vertse, J. Phys. G **36** (2009) 013101 [arXiv:0810.2728 [nucl-th]].
 - [3] J. Meng and S. Zhou, J. Phys. G **42** (2015) 093101 [arXiv:1507.01079 [nucl-th]].
 - [4] T. Berggren, Nucl. Phys. A **109** (1968) 265.
 - [5] T. Berggren and P. Lind, Phys. Rev. C **47** (1993) 768.
 - [6] M. Grasso, N. Sandulescu, N. Van Giai and R. Liotta, Phys. Rev. C **64** (2001) 064321.
 - [7] G. Papadimitriou, J. Rotureau, N. Michel, M. Ploszajczak and B. Barrett, Phys. Rev. C **88** (2013) 044318 [arXiv:1301.7140 [nucl-th]].
 - [8] Z. Sun, Q. Wu, Z. Zhao, B. Hu, S. Dai and F. Xu, Phys. Lett. B **769** (2017) 227.
 - [9] S. Baroni, P. Navrátil and S. Quaglioni, Phys. Rev. C **87** (2013) 034326 [arXiv:1301.3450 [nucl-th]].
 - [10] C. Romero-Redondo, S. Quaglioni, P. Navrátil and G. Hupin, Phys. Rev. Lett. **113** (2014) 032503 [arXiv:1404.1960 [nucl-th]].
 - [11] M. Vorabbi, P. Navrátil, S. Quaglioni and G. Hupin, Phys. Rev. C **100** (2019) no.2, 024304 [arXiv:1906.09258 [nucl-th]].
 - [12] D. Lee, Prog. Part. Nucl. Phys. **63** (2009) 117 [arXiv:0804.3501 [nucl-th]].
 - [13] T. A. Lhde and U.-G. Meißner, Lect. Notes Phys. **957** (2019) 1.
 - [14] E. Epelbaum, H. Krebs, D. Lee and U.-G. Meißner, Phys. Rev. Lett. **106** (2011) 192501 [arXiv:1101.2547 [nucl-th]].
 - [15] S. Elhatisari, D. Lee, G. Rupak, E. Epelbaum, H. Krebs, T. A. Lähde, T. Luu and U.-G. Meißner, Nature **528** (2015) 111 [arXiv:1506.03513 [nucl-th]].
 - [16] M. Lüscher, Commun. Math. Phys. **105** (1986) 153.
 - [17] M. Lüscher, Nucl. Phys. B **354** (1991) 531.
 - [18] J. M. M. Hall, A. C.-P. Hsu, D. B. Leinweber, A. W. Thomas and R. D. Young, Phys. Rev. D **87** (2013) 094510 [arXiv:1303.4157 [hep-lat]].

- [19] J. J. Wu, T. S. Lee, A. Thomas and R. Young, Phys. Rev. C **90** (2014) 055206 [arXiv:1402.4868 [hep-lat]].
- [20] Z. W. Liu, W. Kamleh, D. B. Leinweber, F. M. Stokes, A. W. Thomas and J. J. Wu, Phys. Rev. Lett. **116** (2016) 082004 [arXiv:1512.00140 [hep-lat]].
- [21] J. J. Wu, H. Kamano, T.-S. H. Lee, D. B. Leinweber and A. W. Thomas, Phys. Rev. D **95** (2017) 114507 [arXiv:1611.05970 [hep-lat]].
- [22] Z. W. Liu, J. M. M. Hall, D. B. Leinweber, A. W. Thomas and J. J. Wu, Phys. Rev. D **95** (2017) 014506 [arXiv:1607.05856 [nucl-th]].
- [23] J. j. Wu, D. B. Leinweber, Z. w. Liu and A. W. Thomas, Phys. Rev. D **97** (2018) 094509 [arXiv:1703.10715 [nucl-th]].
- [24] Y. Li, J. J. Wu, C. D. Abell, D. B. Leinweber and A. W. Thomas, Phys. Rev. D **101** (2018) 114501 [arXiv:1910.04973 [hep-lat]].
- [25] D. B. Kaplan, Nucl. Phys. B **494** (1997) 471 [arXiv:nucl-th/9610052 [nucl-th]].
- [26] S. S. Kamalov, E. Oset and A. Ramos, Nucl. Phys. A **690** (2001) 494 [arXiv:nucl-th/0010054 [nucl-th]].
- [27] X. Zhang and J. J. Xie, Chin. Phys. C **44** (2020) 054104 [arXiv:1906.07340 [nucl-th]].
- [28] J. J. Wu, T.-S. H. Lee and B. S. Zou, Phys. Rev. C **85** (2012) 044002 [arXiv:1202.1036 [nucl-th]].